Field Crops Research 121 (2011) 125–135

Contents lists available at ScienceDirect

Field Crops Research

journal homepage: www.elsevier.com/locate/fcr

Exploring remotely sensed technologies for monitoring wheat potassium and phosphorus using field spectroscopy

Agustin Pimstein[a,b], Arnon Karnieli[b], Surinder K. Bansal[c], David J. Bonfil[d,*]

[a] Departamento de Fruticultura y Enología, Facultad de Agronomía e Ingeniería Forestal, Pontificia Universidad Católica de Chile, Av. Vicuña Mackenna, 4860 Santiago, Chile
[b] The Remote Sensing Laboratory, Jacob Blaustein Institutes for Desert Research, Ben-Gurion University of the Negev, 84990, Israel
[c] Potash Research Institute of India, Dundahera Delhi-Gurgaon Road, Gurgaon 122001, Haryana, India
[d] Field Crops and Natural Resources Department, The Institute of Plant Sciences, Agricultural Research Organization, Gilat Research Center, 85280 MP Negev 2, Israel

ARTICLE INFO

Article history:
Received 3 March 2010
Received in revised form 1 December 2010
Accepted 1 December 2010

Keywords:
Wheat
Remote sensing
Field spectroscopy
Potassium
Phosphorus
Vegetation indices
Partial Least Squares regression

ABSTRACT

Given the importance of potassium (K) and phosphorus (P) contents to wheat yield and grain quality, and the very little experience that has been gained on nutritional monitoring of other than nitrogen using remotely sensed technologies, a study was undertaken to explore the possibility of identifying these mineral stresses using spectral data. Canopy spectra and biophysical data were collected from commercial and experimental fields in India and Israel. Traditional and newly developed vegetation indices, together with Partial Least Squares (PLS) regression models, were calculated in order to predict potassium and phosphorus contents from the wheat canopy spectral data. Results show that the application of PLS and specific narrow bands vegetation indices reached significant levels of accuracy in the retrieval of K and P levels, in comparison to traditional broad band indices. Additionally, it was observed that a significant improvement is obtained when the mineral total content is considered instead of the relative content. Therefore it was suggested that the biomass should also be retrieved from the spectral data. Finally, as very different crop conditions were included in this study, it was possible to confirm that the level of accuracy in the retrieval of K and P levels is related to the quality and variability of the data used for calibrating the models.

1. Introduction

The current pressure for optimizing agricultural production, from both economic and environmental points of view, has pushed the industry to adopt more efficient management practices. Besides the development of better and more efficient machinery, the agriculture industry is adopting information technology tools at a very fast pace. Plant and soil sensors, geographic information systems, and satellite and airborne images (remote sensing), are several of these new technologies that farmers, consultants, and researchers are using in order to improve operational efficiency. Until recent years, a large portion of the remotely sensed products that have been used as management tools in agriculture have been based on vegetation indices (VIs) that mainly include the near-infrared and the red spectral bands. Most commonly used is the Normalized Difference Vegetation Index (NDVI), followed by other related VIs (Hatfield et al., 2008). Although this index has been correlated to several crop biophysical parameters, it lacks of sensitivity when applied to crops with high biomass development (Baret and Guyot, 1991; Buschmann and Nagel, 1993; Aparicio et al., 2002). Incorporating multivariate data analysis with spectroscopy data and hyperspectral images has already shown a significant improvement for retrieving quantitative information about the crops (Hansen and Schjoerring, 2003; Nguyen and Lee, 2006; Pimstein et al., 2007). These types of images can be obtained from airborne and spaceborne hyperspectral sensors that collect images with hundreds of narrow spectral bands. A large number of spectral bands might increase the accuracy in characterizing the condition of specific elements of the plant. Additionally, hyperspectral data is also applied for the development of fertilizer equipment, which includes multispectral optical sensors for on-going monitoring (Samborski et al., 2009). However, this technology is still limited to the prediction of nitrogen condition or biomass development (e.g., Cohen et al., 2009; Herrmann et al., 2010; Samborski et al., 2009).

Very little experience has been gained regarding nutritional monitoring in field crops of elements other than nitrogen using remotely sensed data. Preliminary works exhibit the effect of several macro nutrient deficiencies on the reflectance, but were limited to pot experiments in controlled environments (Ponzoni and Goncalves, 1999; Ayala-Silva and Beyl, 2005). Since potassium (K) and phosphorus (P) are the two most important macronutrients required by plants after nitrogen (N), the ability to monitor

* Corresponding author. Tel.: +972 8 9928654; fax: +972 8 9926485.
E-mail address: bonfil@volcani.agri.gov.il (D.J. Bonfil).

0378-4290/$ – see front matter © 2010 Elsevier B.V. All rights reserved.
doi:10.1016/j.fcr.2010.12.001

their status through remote sensing is important. Potassium concentration in wheat plants typically ranges between 1 and 5% and it is absorbed from the soil solution as the ion K^+. Being a mobile element that is translocated to the younger tissues, the deficiency symptoms usually appear first on the lower leaves of annual plants, progressing towards the top as the severity of the deficiency increases (Tisdale et al., 1985). Potassium deficiency results in discoloration of tips and margins of wheat leaves, causing them to turn yellow and brown when the shoot is undergoing its rapid phase of growth. As in other cereal crops, lack of potassium in wheat often also causes weakening of the straw which may result in lodging. Phosphorus, is present in wheat plants in much lower concentrations (0.1–0.4%) than nitrogen and potassium. However, as it is a component of adenosine di- and tri-phosphates (ADP and ATP, respectively), phosphorus directly affects almost every energy-requiring biological process in the plant, e.g. photosynthesis, respiration, membrane transport, and biosynthesis of cell components (Tisdale et al., 1985). In young plants deficient in phosphorus, leaves and stems turn bluish green and develop strong purple tints, while older leaves die off early. At later stages of development, leaves show purplish bronze tints, and spikes do not develop correctly (Wallace, 1943).

Ponzoni and Goncalves (1999) observed that phosphorus deficit in *Eucalyptus saligna* was significantly correlated to leaf green reflectance (~550 nm). However, better correlations were obtained for predicting phosphorus deficiency when considering the N/P relationship. This relationship between nitrogen and phosphorus and also that between nitrogen and potassium, have been confirmed by Ayala-Silva and Beyl (2005) who observed a significant reduction of chlorophyll content in wheat plants when grown in a greenhouse under independent potassium and phosphorus deficits. Due to this significant interaction between nitrogen and phosphorus, together with the important role of phosphorus throughout the entire growth period, phosphorus and potassium deficiencies have been analysed through their effect on crop chlorophyll content. For example, the potassium effect was analysed in barley using the broadband Relative Vegetation Index (RVI, ratio between NIR and the Photosynthetically Active Radiation (PAR)), showing a positive response of biomass growth to potassium fertilization (Petersen et al., 2002). On the other hand, this study showed that RVI correlates well with applied nitrogen, irrespective of potassium application, meaning that RVI's main source of variation corresponds to nitrogen, and is less sensitive to potassium. This opposes what was preliminarily observed in *E. saligna* leaves, where an induced potassium deficit was observed to be a significant factor in the changes in the VIS region, especially the red reflectance (~680 nm). An induced nitrogen and potassium deficit for 10 years in olive trees was able to be discriminated using 26 specific wavelengths plus several vegetation indices (Gomez-Casero et al., 2007). In addition, Osborne et al. (2002) confirmed in corn that the increase in the number of cells per unit of leaf area in phosphorus-stressed plants was translated into a significant spectral response in the NIR part of the spectrum. Specifically, they found that linear models that included 730 and 930 nm, were able to predict phosphorus concentration at one specific timepoint of the crop development (V6, growth stage denoted by the expansion of the sixth leaf). For later development stages, the model for predicting phosphorus concentration included wavelengths located around the blue part of the spectrum (440 and 445 nm), meaning that very specific models are needed for different stages, depending on the differing effect of phosphorus on the crop. For these later stages (V7–V8, expansion of the 7th–8th leaves), phosphorus stress is associated with an increase in anthocyanin, causing a purple discoloration in the leave margins, which matches the observed increase in reflectance at these wavelengths. Despite the existing accumulated knowledge, more specific indices or algorithms are needed for predicting the nutrient condition of potassium and phosphorus.

The objective of this research was to develop a new algorithm for characterizing the potassium and phosphorus contents of wheat (*Triticum aestivum* L.) crop using field spectroscopic data. In order to achieve this goal, canopy reflectance measurements were collected from experimental and commercial fields in India and Israel. Spectral data were analysed and evaluated by existing and proposed vegetation indices, as by Partial Least Squares (PLS) regression models.

2. Materials and methods

2.1. Study area

2.1.1. Dataset 1 – Indian campaign

Between the 23rd and 27th of January of 2007, an intensive field campaign was performed in northern India, collecting samples from an experimental site (28°16′45N, 77°04′05E) and neighboring fields located close to the town of Sohna in the surroundings of Delhi. This area is characterized by loamy sand to sandy loam soil, generally well drained, but with a severe lack of potassium. Annual average precipitation is 455 mm, with daily average minimum and maximum winter temperatures of 11 °C and 24 °C, respectively.

In the experimental site, which is maintained by the Potash Research Institute of India, extra pre-sowing potassium was applied to two fields at a rate of 50 kg K^+ ha^{-1}. These fields were selected by the local manager of the site so to achieve the best crop conditions. This fertilization is unusual to the common wheat growers of the area, so its purpose was to create wider variability among this dataset. In the first day of this campaign, 43 measurements were randomly performed on this experimental site, half from the fertilized fields, and half from the non-fertilized fields. These measurements included spectral reflectance and sampling of all the plants included in the field of view of the spectrometer, for biomass and nutritional analysis. More details about these measurements are discussed in Sections 2.2 and 2.3. During the following days, additional samples were collected from the neighboring fields, usually collecting one sample per field, or a maximum of two in those cases in which differences were clearly distinguished. A total of 128 canopy samples were collected during the five days of measurements, which were harvested for biophysical analysis immediately after the spectral measurements from above the canopy were taken. These samples covered the main development stages of active vegetative growth, spanning from stem elongation to beginning of flowering.

2.1.2. Dataset 2 – Israeli experimental and commercial fields

During the 2005/06 and 2006/07 growing seasons, a large dataset was collected from a wide range of field trials that were held both at the Gilat Research Center (31°20′03N, 34°39′58E) and at commercial fields located in its surroundings. As well as for Dataset 1, these measurements included spectral reflectance and biomass sampling. This semi-arid area is characterized by a mean annual rainfall of 237 mm concentrated in winter, with high interannual rainfall variability and a high oscillation of daily winter temperatures (Bonfil et al., 1999).

The purpose of collecting data from trials that were being held in commercial plots was to simultaneously characterize the real growing conditions in commercial operations, and also to increase variability. Details of some of these experiments were presented in previous works (Pimstein et al., 2007, 2009). These trials included a wide range of seeding densities, varieties, irrigation, and fertilization treatments. A total of 489 canopy samples were collected from these experiments, including samples from the very begin-

Table 1
Vegetation indices.

Vegetation indices	Formula	Reference
Normalized Difference Vegetation Index	$NDVI = \frac{\rho_{800-900} - \rho_{650-700}}{\rho_{800-900} + \rho_{650-700}}$	Rouse et al. (1974)
Green-NDVI	$GNDVI = \frac{\rho_{800-900} - \rho_{540-560}}{\rho_{800-900} + \rho_{540-560}}$	Gitelson et al. (1996)
Simple ratio	$SR = \frac{\rho_{800-900}}{\rho_{650-700}}$	Birth and McVey (1968)
Soil Adjusted Vegetation Index	$SAVI = \frac{\rho_{800-900} - \rho_{650-700}}{\rho_{800-900} + \rho_{650-700} + 0.5}(1 + 0.5)$	Huete (1988)
Optimized Soil-Adjusted Vegetation Index	$OSAVI = \frac{(1 + 0.16)(\rho_{800} - \rho_{670})}{(\rho_{800} + \rho_{670} + 0.16)}$	Haboudane et al. (2002)
Red-Edge position[a]	$REP = 700 + 40 \cdot \frac{\rho_{re} - \rho_{700}}{\rho_{740} - \rho_{700}}$	Guyot and Baret (1988)

[a] ρ_{re} is the red-edge inflection point that corresponds to the interpolation between the reflectance at 670 and 780 nm.

ning of the season (~10 days after emergence, DAE) until heading time (~100 DAE). As for Dataset 1, the samples were harvested for biophysical analysis immediately after the spectral measurements from above the canopy were taken.

2.2. Spectral data

Canopy radiance in India and Israel was measured with the same portable Analytical Spectral Devices (ASD) Field Spec® Pro spectrometer that consisted of a spectral range of 350–2500 nm and a 25° field of view. The spectrometer is equipped with three sensors (visible and near infrared-VNIR, shortwave infrared-SWIR1, and SWIR2) with spectral sampling of 3, 10, and 10 nm, respectively. As the built-in spectral resolution output of the data from the ASD operating system is 1 nm along the whole spectrum, the data were later averaged homogeneously to 5 nm. The atmospheric water absorption spectral regions (1350–1420 and 1800–1960 nm) were masked before analysis. The instrument was periodically calibrated to spectral reflectance using a standard white reference panel (Spectralon Labsphere Inc., North Sutton, NH, USA). Reflectance data were collected at a constant height of 1.5 m above the ground, corresponding to an instantaneous field of view (IFOV) that included an average of almost four rows, at emergence. As the crop height increased through the season, the IFOV above the canopy was reduced proportionally, but included at least two complete rows for all the measurements of both datasets. These measurements were carried out throughout 5 h between 10:00 and 15:00 local time under clear sky conditions, in a nadir orientation. For Dataset 2, this period was strictly kept at 4 h around solar noon. For each sampled plot of the Dataset 1, between four and five spectra for later averaging were collected around the spot that was sampled in the specific field. For Dataset 2, on each sampling date, each measurement was collected from a different homogeneous point in each plot. During the Indian campaign, leaf reflectance was collected over a black polyethylene background, using the ASD halogen bulb High Intensity Contact Probe. For this case, four flag leaves (or the most extended one) were measured and then averaged for characterizing the leaf spectrum of each collected sample. Despite that the reflectance measurement takes only a couple of seconds and the leaves are not damaged by the probe's light, these precise leaves were not included in the laboratory analysis.

2.3. Biophysical variables

Samples for the determination of biophysical variables (biomass, and N–P–K total concentration based on dry weight) were collected within a 60 cm × 50 cm frame (0.3 m^2). The dry biomass was measured after drying for 48 h at 70 °C. After drying the samples, the material from the whole plant was ground and mixed, and sub-samples were weighed and set apart for nutrient analysis. N concentration was obtained using the micro-Kjeldhal method (Jones and Case, 1990). Phosphorus and potassium were extracted by the di-acid (HNO_3–$HClO_4$) wet digestion method. After extraction, phosphorus content was estimated on a Spectronic-20 Spectrophotometer at 420 nm, while potassium estimation was performed on an EEL-Corning flame-photometer.

Based on the results of Ayala-Silva and Beyl (2005) in wheat, who discussed a significant correlation of the response between chlorophyll content and K, the ratio between the concentration of N and K were also computed and considered as an additional variable. Additionally, the total amount of nutrients was also estimated by multiplying their concentration by the dry biomass, resulting in weight-based new variables (Nw–Pw–Kw).

2.4. Data analysis

2.4.1. Spectral analysis

Dataset 1 was used to identify, on a preliminary basis, the direct effect of potassium and phosphorus deficiency on the spectral response of wheat plants in order to examine new vegetation indices.

To identify the nutrients' effect on the crop's spectral response, the reflectance at each wavelength, both for the canopy and leaf level, were correlated with the biophysical variables. This was computed through simple correlation of two vectors, one corresponding to the reflectance of all the samples of a specific wavelength (one at a time), and the second one to the values of the biophysical variables. The latter vector was kept the same for the analysis of each wavelength. During this calculation, in order to identify significant wavelengths, a p-value of 5% of confidence was also computed.

2.4.2. Vegetation indices

Traditional vegetation indices (Table 1) were evaluated as a potential tool for monitoring the crop nutritional contents by quantitatively retrieving the nutrient content in the crop. Additionally, based on the outcomes of the spectral analysis (Section 2.4.1), two newly proposed vegetation indices were also evaluated. Two approaches were followed for developing these new indices (i) index with a normalized structure that considers one wavelength with the same degree of correlation for both potassium and nitrogen, and the other wavelength with a different degree of correlation and (ii) a normalized index whose wavelengths will be searched among all the possible wavelengths combination, and then comparing their relationship with the potassium and phosphorus concentration of Dataset 1.

The capability of these VIs to quantitatively retrieve the potassium and phosphorus content of the crop was calculated independently in Dataset 1, Dataset 2, as well as in the combination of both. For each of these three scenarios a calibration subset of 2/3 of the data was randomly selected for developing linear models that were later applied on the remainder 1/3 of the data (validation subset). Additionally, the models developed from

Table 2
Biophysical variables statistics of Dataset 1 & 2.

Dataset		Dry biomass ($g\,m^{-2}$)	N (%)	P (%)	K (%)
DS1[a] – canopy	Min–Max	101–401	1.47–2.61	0.30–0.39	1.34–2.46
($N = 128$)	Mean (STD[b])	251 (62)	2.08 (0.22)	0.334 (0.017)	1.92 (0.24)
	CV[c](%)	25	10.43	5.180	12.67
DS1 – Leaves	Min–Max	83–392	1.49–2.46	0.301–0.358	1.41–2.31
($N = 18$)	Mean (STD)	166 (81)	1.94 (0.30)	0.321 (0.017)	1.70 (0.22)
	CV (%)	49	15.61	5.309	13.05
DS2 – canopy	Min–Max	3.8–1440	0.77–4.71	0.04–0.47	0.75–4.58
($N = 489$)	Mean (STD)	359 (277)	2.90 (0.96)	0.280 (0.075)	2.97 (0.74)
	CV (%)	77	33.10	26.741	25.06
DS1 and DS2	Min–Max	3.8–1440	0.77–4.71	0.04–0.47	0.75–4.58
Canopy	Mean (STD)	336 (252)	2.71 (0.92)	0.291 (0.071)	2.75 (0.79)
($N = 618$)	CV (%)	75	33.88	24.236	28.85

[a] DS: dataset.
[b] STD: standard deviation.
[c] CV: coefficient of variation (STD/Mean).

Dataset 1 were validated on Dataset 2. The statistics, Root Mean Square Error of Prediction (RMSEP) and correlation coefficient (R) were calculated to compare the accuracy obtained by each of the VIs.

2.4.3. Multivariate data analysis

For the multivariate data analysis procedure, The Unscrambler ver. 9.7 software (developed by CAMO Software AS – www.camo.com) was used to define different models and to predict biophysical data. The biophysical data were considered as response variables and the spectral data, as the explanatory variables. Partial Least Squares (PLS) regression was used to find the best prediction of the biophysical variables. These regression models were obtained by using two-thirds of the dataset, randomly selected, as a calibration subset. Based on previous experience (Pimstein et al., 2007), the PLS analysis was applied only to the 1st derivative of the reflectance, and the selection of the significant wavelengths using the Unscrambler built-in tool as only pre-processing. Validation was performed by predicting the remaining one-third of the dataset that formed the validation subset. RMSEP and R were calculated to compare the accuracy between the models and to have another indicator to compare with the previously analysed VIs.

3. Results and discussion

3.1. Biophysical variables

As mentioned, the measurements performed during this research included canopy reflectance and subsequent laboratory analysis of the collected samples (dry biomass and nutritional content of nitrogen, phosphorus, and potassium). The statistics of the measured biophysical variables for each dataset (based on laboratory analysis) are presented in Table 2. In addition, the statistics for the leaves subset of Dataset 1 and for the combination of Dataset 1 + 2 are included. Table 2 confirms what was originally stated about the lower potassium levels in the Indian samples in comparison to the Israeli samples. This is illustrated by the significantly higher potassium mean content of Dataset 2 that had never received potassium fertilization. Part of Dataset 1 variation can be explained by the fact that the fields were managed by different growers, at slightly different soil conditions, and were seeded on slightly different dates, etc. The potassium variability in Dataset 1 was slightly increased by the extra pre-sowing potassium application in two fields (29 from the overall 128 samples). The rest of the samples from this experimental site, as well as those that

Table 3
Cross-correlation (R) between the biophysical variables, based on all the samples of Dataset 1 ($n = 128$), Dataset 2 ($n = 489$) and Dataset 1 + 2 ($n = 617$).

	Dry biomass	N	P	K	Nw	Pw	Kw
Dataset 1							
Dry biomass	1						
N	0.82	1					
P	0.59	0.53	1				
K	0.70	0.65	0.52	1			
Nw	0.98	0.90	0.60	0.72	1		
Pw	0.96	0.81	0.61	0.87	0.96	1	
Kw	0.99	0.82	0.71	0.72	0.97	0.96	1
Dataset 2							
Dry biomass	1						
N	−0.81	1					
P	−0.44	0.57	1				
K	−0.57	0.79	0.56	1			
Nw	0.86	−0.56	−0.27	−0.26	1		
Pw	0.87	−0.62	−0.28	−0.20	0.95	1	
Kw	0.93	−0.71	−0.17	−0.41	0.89	0.90	1
Dataset 1 + 2							
Dry biomass	1						
N	−0.67	1					
P	−0.45	0.40	1				
K	−0.36	0.81	0.29	1			
Nw	0.87	−0.40	−0.31	−0.06	1		
Pw	0.87	−0.44	−0.33	0.01	0.95	1	
Kw	0.92	−0.61	−0.16	−0.29	0.88	0.87	1

were collected from the neighboring fields, did not receive any supplemental potassium.

Finally, when analysing both datasets together (Dataset 1 + 2) it can be noticed that Dataset 2 corresponds to a larger percentage of this "new" whole dataset. However, the advantage of considering this whole dataset is the fact that very important samples of low potassium content during heading time (from Dataset 1) are included, expanding the range of influence of any developed model.

In addition to the biophysical variability, before selecting a specific dataset for analysing the correlation between spectra and their biophysical characteristics, it is important to consider the cross-correlation between these parameters. Plant nutrient contents are often highly correlated, especially when considering data that covers the entire growing period. Therefore, for wavelength selection it is important to consider a dataset from a specific moment of the season in which the cross-correlation between the nutrients is low. This was the purpose of using only Dataset 1 for selecting the wavelengths, because as can be seen in Table 3, the cross-correlation between N–P–K, especially nitrogen and potassium, is lower than the one obtained for Dataset 2. As expected, there is a high correlation between dry biomass and nitrogen concentration. The fact that this correlation is positive for Dataset 1 and negative for Dataset 2 (and obviously also for the combined Dataset 1 + 2), confirms that the fields in India were still growing and the nitrogen was still accumulating, while the Israeli dataset includes fields from the whole season, limiting its applicability for selecting wavelengths for spectral indices.

3.2. Nutrient spectral response

Leaf reflectance showed the classical vegetation spectrum with strong chlorophyll absorption in the blue and red bands (460 and 660 nm, respectively), amplified reflectance caused by the leaf structure in the NIR parts of the spectrum, and the shortwave infrared (SWIR) characteristic water absorption features. In order to explore the wavelengths that could be used for monitoring the nutrient status of the whole plant, correlation analysis was performed between leaf and canopy reflectance, and the whole plant N–P–K concentration levels (Fig. 1).

As can be observed, the absolute values of the correlation coefficients along the spectrum are quite similar between the canopy and leaf levels, being slightly higher in some specific sections for the leaf level; in VIS and NIR range for nitrogen and in SWIR for phosphorus. However, due to the much smaller number of samples at the leaf level, its level of significance is set at a much higher value, limiting the possibility of accurately characterizing the nutritional status of the whole plant by the leaf reflectance. Therefore, besides the VIS wavelengths that show significance for the nitrogen concentration, no significant wavelengths were identified at the leaf level for phosphorus or potassium (Fig. 1a). Despite the lack of significance between potassium and leaf reflectance, it is interesting to see that in a major part of the spectrum, the potassium correlation followed a similar pattern to the nitrogen correlation, suggesting some cross-correlation involving these two elements at the leaf level. Regarding the relationship between phosphorus and leaf reflectance (Fig. 1a), it can be seen that only between 1400–1500 nm and 1900–2100 nm phosphorus shows a stronger correlation than the one obtained for nitrogen, thus these could be potential regions for a phosphorus-based vegetation index.

From Fig. 1b it can be observed that at the canopy level, the whole VIS and SWIR part of the spectrum have significant correlations with the three analysed biophysical variables. This confirms that the low amount of significant wavelengths identified from the leaves spectra was influenced by the small sampled number. Interesting to see is the fact that potassium and phosphorus follow the same correlation pattern as nitrogen, potassium and nitrogen being

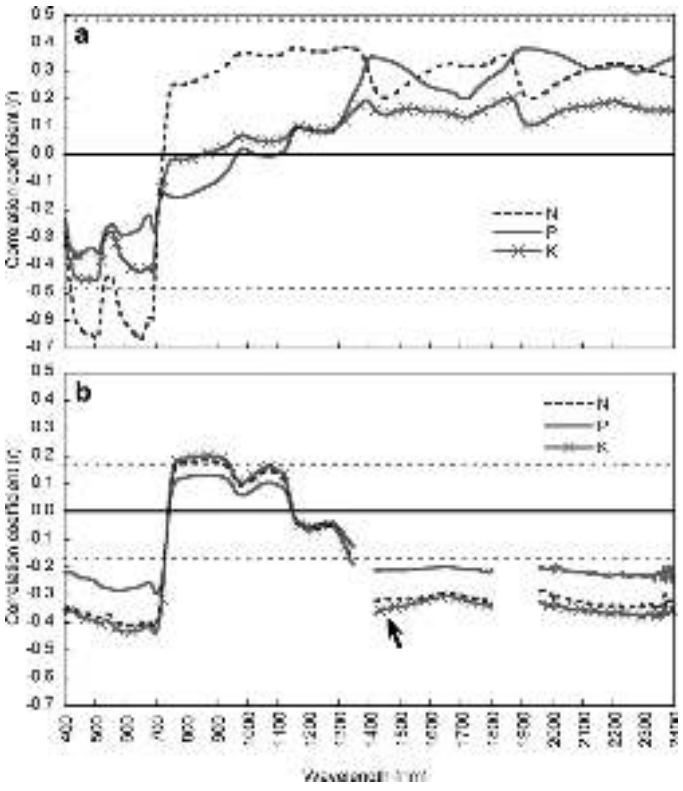

Fig. 1. Correlation coefficient (R) between whole plant N–P–K concentration and leaves reflectance (a), and canopy reflectance (b) from Dataset 1. Dotted horizontal lines illustrate significance level (p-value < 0.05).

the ones with the highest degree of confidence. Therefore, considering the widely reported strong relationship between nitrogen concentration and canopy reflectance (e.g., Knipling, 1970; Bowker et al., 1985; Curran, 1989; Filella et al., 1995; Seelan et al., 2003), this almost identical relationship between potassium and nitrogen and reflectance suggests the need to include a new biophysical parameter (N/K) in the analysis. Considering the mobility of the K^+ ion, this N/K indicator is of special interest as it can identify deficit of the crop when the younger leaves still do not express symptoms of potassium stress in the plant. Therefore, by relating both nitrogen and potassium, a better representation of the crop nutritional condition is obtained.

Additionally, Fig. 1b shows that in addition to what was observed at the leaf level, the canopy reflectance correlation to potassium at 1450 nm is even higher than the one observed for the other wavelengths. These findings set the basis for a possibility that, an index considering this spectral zone could lead to good differentiation between potassium and nitrogen stress. However, it must be taken into account that this wavelength is too close to a water absorption band, making it possible that when collecting data from an airborne or spaceborne platform, it could be affected adversely by atmospheric moisture.

Based on the outcomes of this correlation analysis, a new vegetation index is proposed, that includes a basic wavelength with the similar correlation coefficients for both potassium and nitrogen (870 nm), and one with different correlation coefficients (1450 nm). In order to enhance the differences between the wavelengths and to obtain positive values, the normalized configuration was selected, as presented in Eq. (1).

$$\mathrm{N\_870\_1450} = \frac{\rho_{870} - \rho_{1450}}{\rho_{870} + \rho_{1450}} \quad (1)$$

where ρ represents the reflectance at the respective wavelength.

In addition, an alternative VI was evaluated by combining all the wavelengths using the same normalized structure of Eq. (1), and then comparing their values with the potassium and phosphorus concentration of Dataset 1. The wavelengths that resulted in the best combination for both potassium and phosphorus were 1645 nm and 1715 nm (Eq. (2)). One of the advantages of this combination is the fact that these wavelengths are located out of the water absorption regions and are usually included among the spectral bands of airborne hyperspectral images.

$$N\_1645\_1715 = \frac{\rho_{1645} - \rho_{1715}}{\rho_{1645} + \rho_{1715}} \quad (2)$$

3.3. Quantitative retrieval of potassium and phosphorus

3.3.1. K and P retrieval with vegetation indices

Table 4 shows that only for Dataset 1, the models developed for both nutrients resulted in acceptable levels of accuracy when testing them in its own validation subsets. Specifically for this dataset, the higher potassium variability among the samples (Table 2) in comparison to the phosphorus explains the stronger results for potassium, enhancing the importance of the variability of the calibration dataset in order to get acceptable models. This accuracy in the prediction was significantly reduced when the developed models (from Dataset 1) were used for predicting potassium and phosphorus from Dataset 2 (2nd section of Table 4). This confirms the need of very similar values spread (range) to make these indices work correctly. Moreover, due to the extreme different conditions of both datasets, the predicted values applying all the VIs resulted in an inverse relationship with the measured values. The importance of the calibration samples' variability is enhanced when comparing Dataset 1 with Dataset 2 results. As shown in Table 4 (3rd section), only N_1645_1715 provides significant prediction of potassium based on the models developed from its own calibration subset. No index provided significant accuracy in the prediction of phosphorus for this dataset. The predictions calculated with the rest of the indices are not significant, and in fact it can be said that although the potassium prediction was statistically significant, it does not provide enough level of accuracy to be considered as applicable. This lack of sensitivity of the VIs for developing an acceptable model for Dataset 2 is explained by their large dispersion along the nutrient concentration or lack of sensitivity. From the last section of Table 4, it can be seen that although more VIs are significant when analysing all the data together (Dataset 1 + 2), they are still not applicable. The poor response of these VIs when Dataset 2 is included could be related to the high effect of the dry biomass variability. Interesting to see in Table 2 that in Dataset 1 the biomass coefficient of variation (CV) is twice the potassium concentration CV, while in Dataset 2 and in the combined Dataset (1 + 2), the biomass CV is three times higher. A similar situation is observed when comparing the biomass CV with the phosphorus concentration CV in Dataset 1, which is almost five times larger, and also the VIs showed relatively low levels of accuracy. These findings suggest that more important than the variability of the variable of interest, is its relationship with the biomass variability. In summary, when the biomass variability increases, it masks the potassium and phosphorus variation, and phosphorus/potassium prediction can be done only through the total potassium and phosphorus content.

Table 4
Retrieval accuracy (R/RMSEP) of phosphorus and potassium concentration obtained by applying linear models of the vegetation indices.

VI	P	K
Cal: Calibration subset DS 1 (n = 85); Val: validation subset DS 1 (n = 43)		
NDVI	0.32/0.018	0.57/0.217
GNDVI	0.36/0.018	0.61/0.212
SR	0.31/0.018	0.52/0.223
SAVI	ns	0.46/0.229
OSAVI	ns	0.50/0.225
REP	0.42/0.018	0.64/0.208
N_1645_1715	0.55/0.017	0.73/0.194
N_870_1450	ns	0.52/0.222
Cal: Calibration subset DS 1 (n = 85); Val: Whole DS 2 (n = 489)		
NDVI	ns	−0.13/1.436
GNDVI	ns	−0.16/1.393
SR	ns	−0.15/1.343
SAVI	ns	ns
OSAVI	ns	ns
REP	−0.15/0.093	−0.13/1.329
N_1645_1715	−0.28/0.098	−0.31/1.280
N_870_1450	ns	−0.15/1.424
Cal: Calibration subset DS 2 (n = 327); Val: validation subset DS 2 (n = 163)		
NDVI	ns	ns
GNDVI	ns	ns
SR	ns	ns
SAVI	ns	ns
OSAVI	ns	ns
REP	ns	ns
N_1645_1715	ns	0.22/0.69
N_870_1450	ns	ns
Cal: Calibration subset DS 1 + 2 (n = 412); Val: validation subset DS 1 + 2 (n = 206)		
NDVI	ns	0.22/0.783
GNDVI	ns	0.22/0.784
SR	ns	0.18/0.790
SAVI	ns	ns
OSAVI	ns	0.17/0.792
REP	ns	ns
N_1645_1715	0.31/0.068	0.143/0.795
N_870_1450	ns	0.24/0.781

When comparing the accuracy of the analysed indices from Dataset 1 (1st section of Table 4), it can be observed that N_1645_1715 corresponds to the most robust index. The higher slope that can be seen of the potassium calibration function in comparison to the phosphorus relationship (Fig. 2), explains the better accuracy for potassium on Dataset 1.

Based on previous experience with spectral data of field crops, the biomass represents a key factor in canopy reflectance (Stanhill et al., 1972; Pimstein et al., 2009). Earlier works also suggested that when monitoring potassium and/or phosphorus soil conditions, the results correspond to the nitrogen response that directly affects the biomass development (Ponzoni and Goncalves, 1999; Petersen et al., 2002; Ayala-Silva and Beyl, 2005). As already discussed, this relationship influenced the similar spectral response between these nutrients and the crop spectra (Fig. 1b). Therefore, the accuracy of the VIs was also evaluated for the retrieval of the N/K relationship and of total potassium (Kw) and phosphorus (Pw) on a weight basis (dry weight X nutrient concentration). As can be seen from Table 5, the prediction accuracy significantly increased when considering these new variables in comparison to the nutrient concentration (Table 4). As expected, the accuracy obtained for the weight-based variables is similar to the one obtained for the biomass prediction, showing that biomass plays an important role in this high accuracy of the proposed VIs. However, the higher accuracy of N_1645_1715 among Dataset 1 for Kw retrieval (R = 0.74) in comparison for dry biomass (R = 0.67), confirms its ability of characterizing the K condition and also the biomass. Additionally, it is interesting to notice that, confirming the latter; the correlation coefficient of N_1645_1715 for predicting potassium concentration from Dataset 1 (1st section of Table 4) is also higher than the one obtained for dry biomass (0.73 vs. 0.67). It is strange to notice from Table 5 that when fitting specific models for Dataset 1, not a single VI gave significant results when predicting their validation subset of N/K, but when applying these models in Dataset 2, high correlation with relatively low error was obtained (R ~0.70 and RMSEP ~0.20% for N_1645_1715 and REP). This is explained by the small

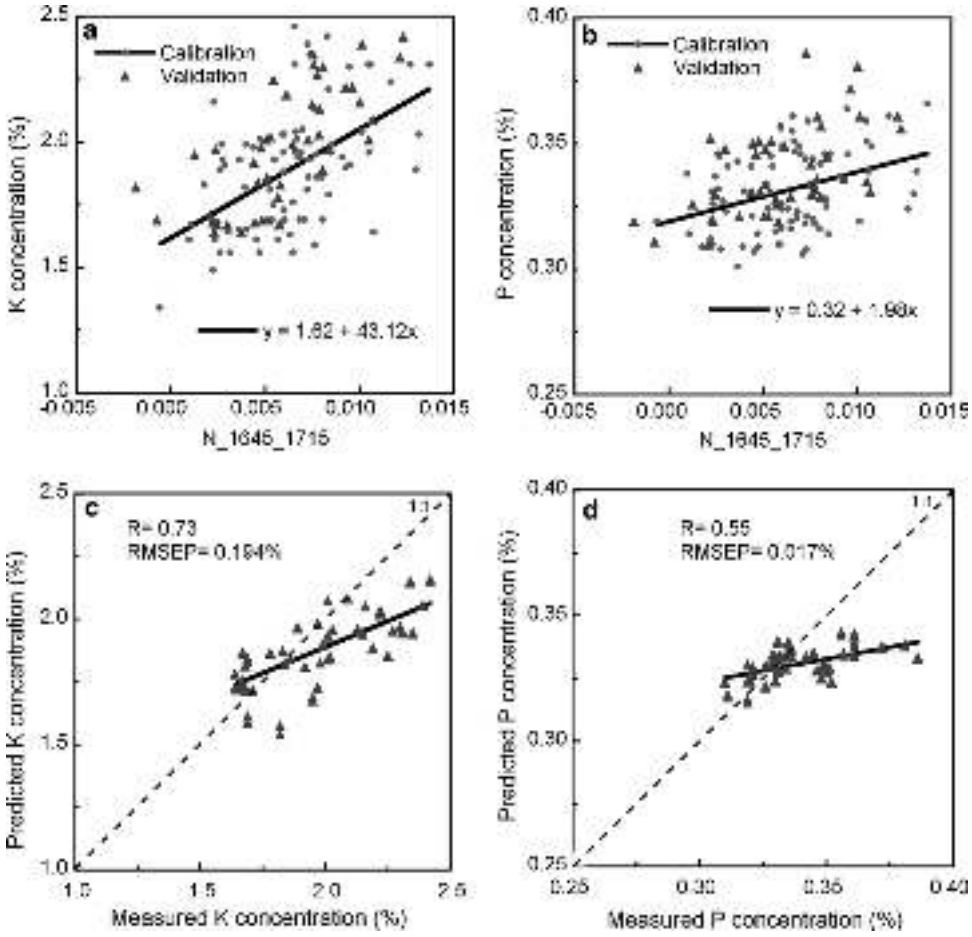

Fig. 2. Linear N_1645_1715 models for K (a) and P (b) concentration based on the calibration subset; validation subset is also shown. (c) and (d) show the relationship between measured and predicted for K and P using the previous models.

range of N/K values obtained in Dataset 1 that limits any possibilities of good predictions by VIs. However, its general trend suits Dataset 2, allowing a good fitting of its model (Fig. 3). If the calibration model of Dataset 1 is extrapolated at larger and smaller values, it will cover most of the range of Dataset 2 and will be able to correctly predict values that were beyond the calibration data. The lack of ability to predict data from its own dataset (validation subset of Dataset 1) is explained by its relatively low nitrogen variability that limited the N/K variability.

When considering all the data together, i.e., the combination of Dataset 1 and 2, the models include samples from different conditions, making them much more robust than the specific ones. From this combination, it can be seen that again REP and N_1645_1715 were the VI that showed the highest correlation coefficient for all

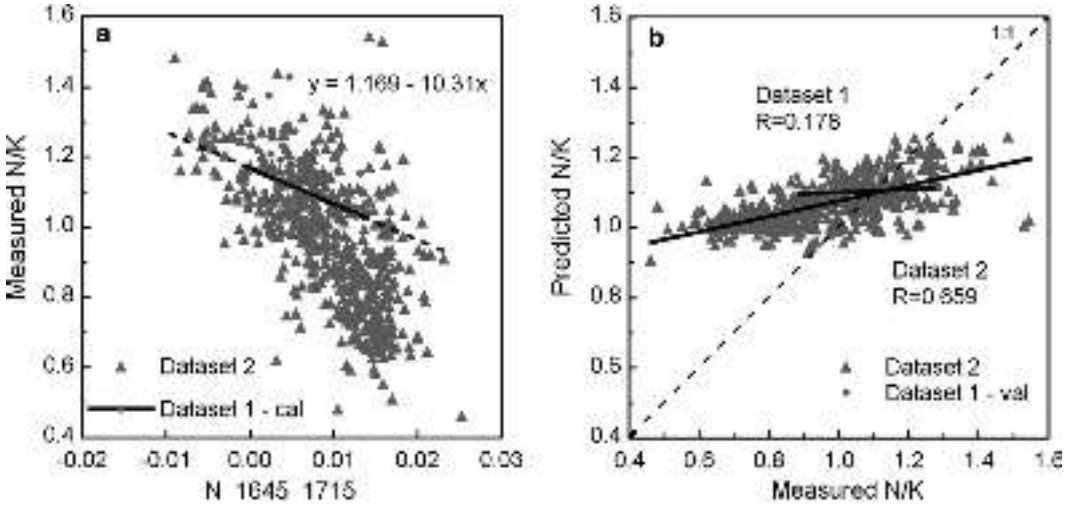

Fig. 3. Linear relationship of the calibration subset of N_1645_1715 VI of Dataset 1 and the whole Dataset 2 for N/K (a), dotted line illustrate extrapolation of linear calibration model; and the validation subset (b) measured vs. predicted N/K using the linear model.

Table 5
Retrieval accuracy (*R*/RMSEP) of dry biomass, weight-based phosphorus (Pw) and potassium (Kw), and N/K relationship by applying linear models of the vegetation indices.

VI	Dry Biomass	Pw	Kw	N/K
Cal: Calibration subset DS 1 (n = 85); Val: Validation subset DS 1 (n = 43)				
NDVI	0.61/51.3	0.58/0.208	0.61/1.414	ns
GNDVI	0.62/51.1	0.59/0.205	0.63/1.385	ns
SR	0.47/56.3	0.47/0.221	0.51/1.501	ns
SAVI	0.46/56.9	0.45/0.224	0.48/1.539	ns
OSAVI	0.53/54.4	0.51/0.217	0.54/1.489	ns
REP	0.60/51. 7	0.60/0.203	0.64/1.366	ns
N_1645_1715	0.67/48.9	0.69/0.192	0.74/1.263	ns
N_870_1450	0.56/53.6	0.52/0.216	0.55/1.477	ns
Cal: Calibration subset DS 1 (n = 85); Val: Validation subset DS 2 (n = 489)				
NDVI	0.59/279.4	0.67/0.556	0.66/7.868	0.55/0.239
GNDVI	0.66/267.8	0.73/0.517	0.73/7.554	0.59/0.238
SR	0.65/280.9	0.80/0.562	0.74/7.812	0.57/0.241
SAVI	0.59/272.8	0.69/0.538	0.72/7.508	0.59/0.239
OSAVI	0.58/276.4	0.67/0.544	0.68/7.692	0.56/0.239
REP	0.76/250.7	0.83/0.468	0.87/6.967	0.69/0.236
N_1645_1715	0.80/234.4	0.80/0.472	0.80/6.288	0.66/0.195
N_870_1450	0.61/280.1	0.69/0.555	0.67/7.904	0.56/0.240
Cal: Calibration subset DS 2 (n = 327); Val: Validation subset DS 2 (n = 163)				
NDVI	0.62/204.9	0.66/0.503	0.66/5.117	0.61/0.160
GNDVI	0.68/190.8	0.72/0.465	0.72/4.671	0.65/0.153
SR	0.73/181.6	0.81/0.396	0.77/4.343	0.62/0.158
SAVI	0.63/203.3	0.69/0.484	0.72/4.699	0.65/0.153
OSAVI	0.62/206.1	0.67/0.499	0.68/4.993	0.62/0.158
REP	0.78/164.1	0.81/0.393	0.88/3.249	0.75/0.135
N_1645_1715	0.77/166.9	0.76/0.436	0.77/4.311	0.75/0.139
N_870_1450	0.66/198.4	0.70/0.482	0.68/5.001	0.64/0.156
Cal: Calibration subset DS 1 + 2 (n = 412); Val: Validation subset DS 1 + 2 (n = 206)				
NDVI	0.53/221.3	0.64/0.452	0.56/5.110	0.45/0.170
GNDVI	0.59/209.5	0.70/0.420	0.64/4.772	0.50/0.165
SR	0.56/215.6	0.73/0.401	0.61/4.861	0.46/0.169
SAVI	0.55/217.4	0.68/0.433	0.65/4.681	0.49/0.166
OSAVI	0.53/221.4	0.65/0.448	0.59/4.977	0.46/0.169
REP	0.72/180.2	0.81/0.346	0.81/3.642	0.63/0.148
N_1645_1715	0.79/158.2	0.78/0.366	0.80/3.694	0.69/0.138
N_870_1450	0.53/221.1	0.65/0.451	0.55/5.144	0.45/0.170

the analysed variables (4th section of Table 5). Fig. 4 shows that when analysing N_1645_1715 for Kw and Pw, the calibration samples follow some sort of exponential trend, but the deviation of the samples from the function is too high. For this reason, if applying the exponential function to samples with high VI values, small differences will generate very high differences in the predicted values. Therefore, although the linear function also generates higher error at the lower VI values, the overall error is lower than when applying the exponential function (data not shown).

In general, it was observed that there was an improvement in the accuracy of the prediction of potassium and phosphorus when considering total potassium and phosphorus content (Kw and Pw) instead of their concentration. This demonstrates that, as found for barley (Petersen et al., 2002), there is a strong effect of the biomass in the spectra and in all derived VIs. The similar correlation coefficients that were obtained for both the dry biomass and the weight-based variables, for all the cal/val combinations coincides with the high correlation between biomass and the weight-based variables (Table 3). The lack of correlation between the nutrient concentration and nutrient total content raises the need to apply an additional index to retrieve first the biomass from the spectral data, and then the potassium concentration. Additionally, large accuracy differences were observed between the different VIs, N_1645_1715 and REP being the ones that showed the best results. The good response of REP to weight-based potassium corroborates previous results in cotton, where it was observed that under adequate nitrogen availability, REP showed a shift of up to 5 nm to shorter wavelengths on plants under potassium stress (Fridgen and Varco, 2004). This could be an outcome of the leaf reflectance in that wavelength, that exhibits variation in response to N and K (Fig. 1a). Similar trends, but with lower degree of accuracy were the predictions of Pw and N/K. The limitation of using these indices is their very narrow wavelengths, restricting its current application only to hyperspectral images. However, these findings set the possibility of including these wavelengths in future platforms as the REP wavelengths have already been included in the superspectral resolution satellites planned to be launched in the near future (e.g., VENμS, SENTINEL-2).

3.3.2. K and P retrieval with PLS models

As for the VI analysis, PLS models were built for dry biomass, potassium and phosphorus concentration, and for the weight-based variables (Kw–Pw) for the same calibration/validation combinations. Based on previous results (Pimstein et al., 2007), it was decided to consider only the first derivatives and selection of the most significant wavelengths as data pre-processing. Despite that Pimstein et al. (2007) showed that eliminating the outliers can increase the accuracy of the models, due to the different sample number and the strong differences between the datasets, all the samples were considered for the different models. As can be seen from Table 6, PLS models reached higher levels of accuracy than VIs, being especially significant for the nutrient concentration. Comparatively, the improvement of the accuracy in the prediction of the dry biomass and the weight-based variables was smaller. Regarding the variability of the datasets, it can be observed that for the case when a very large and heterogeneous dataset was included (Dataset 2 or Dataset 1 + 2), PLS were able to develop much better models than the ones obtained when considering VIs. However, when applying a model that was developed under specific conditions (e.g., Dataset 1) on different data (e.g., Dataset 2), the accuracy of the prediction was also very limited. This confirms that even for PLS approach the model must be applied to a dataset of similar characteristics to the calibration dataset due to the PLS limitation to extrapolate non-available conditions. Besides the differences in the accuracy obtained by the specific models in comparison to the more general ones, it can be observed from Fig. 5 that for these most specific conditions (Dataset 1) a lower amount of wavelengths were used to obtain the best model. In fact, it can be observed that the models for the larger dataset (DS2 and DS1 + DS2) considered a larger amount of wavelengths. However, wavelength reduction is not necessarily positive, as proves the result of the phosphorus concentration model of Dataset 1 that used a less amount of wavelengths but resulted in low accuracy. Additionally from Fig. 5 a slight difference can be observed between the models for the concentration in comparison to the ones for the total content. As can be seen more specifically for the models of Dataset 1, more wavelengths in the VNIR range were considered given the need to include this area to characterize the biomass content.

As observed for the VIs, the retrieval of the weight-based indicators resulted in better accuracy than for the percentage based indicators. However, as for potassium the direct concentration estimation was of high accuracy, when including the biomass in the comprehensive model (DS1 + DS2), only a relatively small improvement was achieved.

The final decision of what kind of model to use depends on the specificity of the data that is intended to be monitored. This means that if the intention is to monitor a crop at different stages of development, it is recommended to consider a model whose calibration is based on measurements collected throughout the entire season. On the other hand, if only one specific phenological stage is of main interest, the obvious decision is to consider building models based on measurements collected on that specific phenologic stage. A detailed analysis of the results obtained with the model that included both datasets shows that the potassium and phosphorus

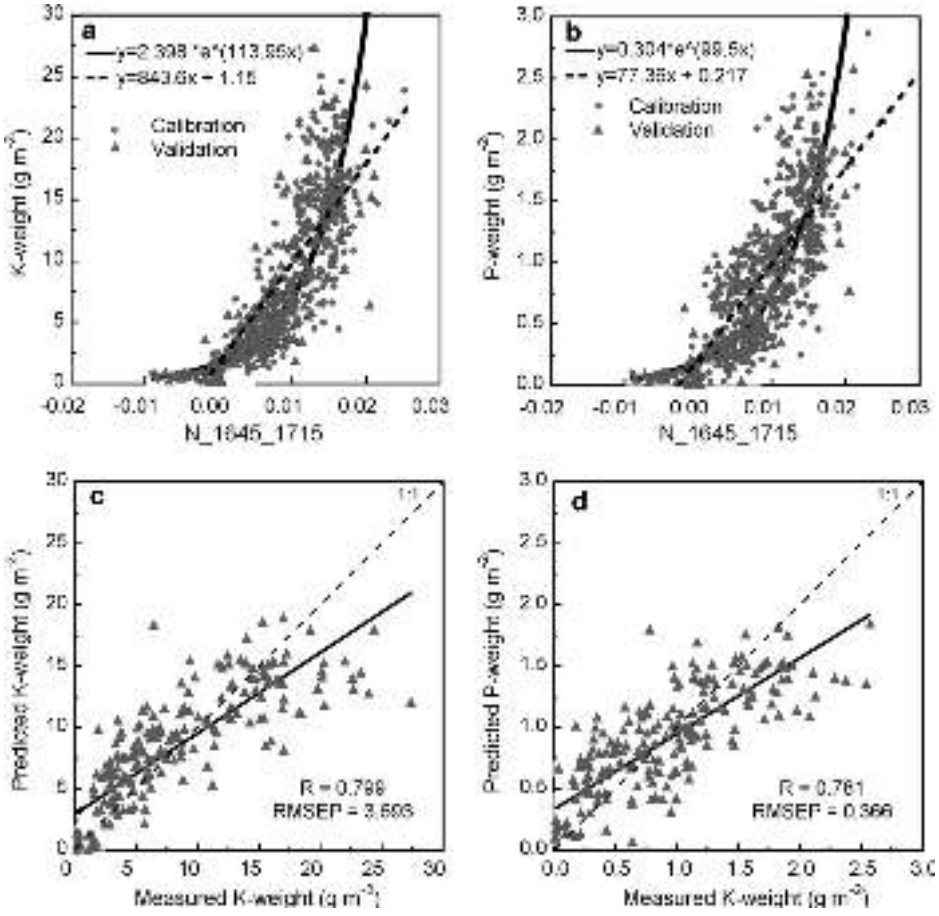

Fig. 4. Weight-based potassium (a) and phosphorus (b) linear and exponential models using N_1645_1715 VI. Validation (c & d) was performed using the linear model.

Table 6
Partial Least Squares regression models accuracy (*R*/RMSEP) for the analysed biophysical parameters, by dataset combinations.

Cal. subset	Val. subset	Dry biomass	P%	K%	Pw	Kw
DS1 (cal.)	DS1 (val.)	0.70/47.5	0.42/0.017	0.69/0.197	0.71/0.178	0.76/1.175
DS1 (cal.)	DS2 (whole)	0.84/174.0	−0.27/0.107	−0.47/1.415	0.90/0.387	0.80/5.017
DS2 (cal.)	DS2 (val.)	0.90/127.2	0.61/0.062	0.88/0.369	0.91/0.274	0.90/2.917
DS1 + 2 (cal.)	DS1 + 2 (val.)	0.90/112.15	0.68/0.054	0.87/0.420	0.90/0.256	0.90/2.705

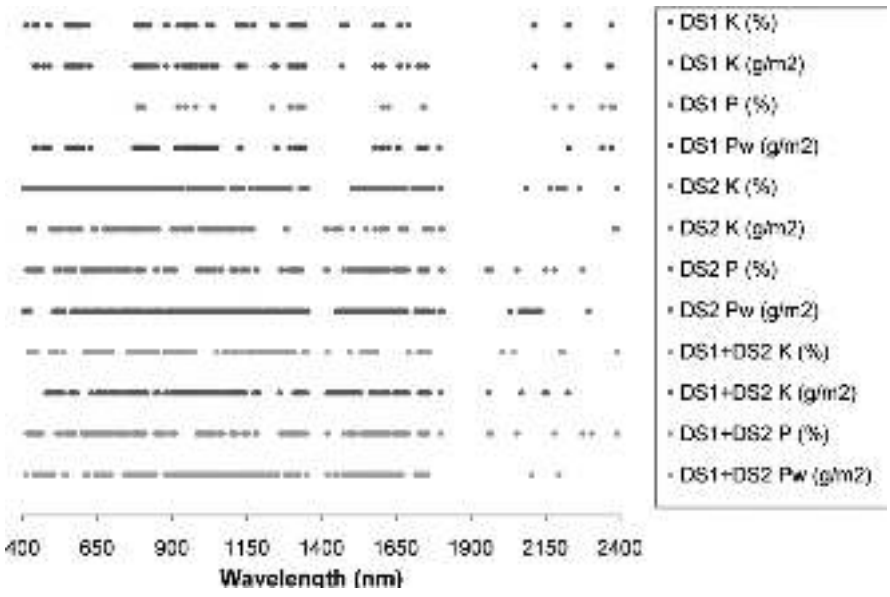

Fig. 5. Selected wavelengths for each of the considered PLS models and datasets combination.

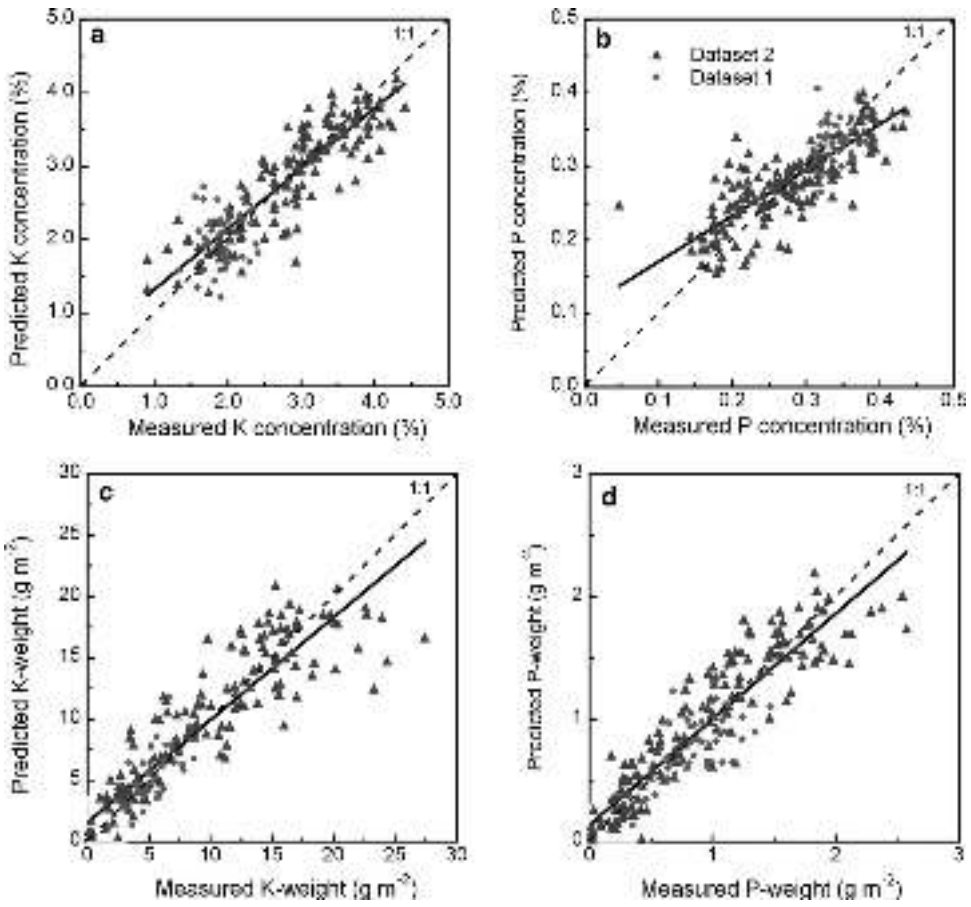

Fig. 6. Accuracy assessment of PLS combined Dataset 1 + 2 models on validation subset. Potassium (a & c), phosphorus (b & d), concentration (a & b), weighted (c & d).

concentration models were able to correctly predict Dataset 2, but large errors are obtained for Dataset 1 (Fig. 6a and b). However, Dataset 1 is only a small part of Dataset 2 for potassium and phosphorus concentration and they integrate smoothly within it. It is important to note that in this study, different wheat cultivars were considered, growing under different growth conditions, in different countries, and were successfully joined to one comprehensive model. Nevertheless, if taking into consideration an indicator that can also reflect the changes during the season (e.g. Kw, Pw), a general model for the entire season will be able to monitor the crop even at specific phenological stages (Fig. 6c and d). This confirms once again the strong effect of the biomass in the spectral response of crop canopies.

4. Conclusions

Based on the current experiments and observations it can be concluded that monitoring potassium and phosphorus contents of wheat crops can be performed using remotely sensed data. However, the level of accuracy and the type of information that can be retrieved depend on the type of sensor and algorithm to be used, as well as on the kind of monitoring that is required to be implemented. Potassium concentration can be retrieved with high levels of accuracy using PLS models, considering both data from a constrained period of the season or from the entire growing period. The application of PLS models is limited by the fact that they require reflectance data along the entire energetic spectrum. On the other hand, potassium concentration can be also be retrieved using the proposed N_1645_1715 index when the potassium and biomass variability of the model calibration samples are similar to the variability of the samples in which the model is going to be applied. Based on the different biomass and nutrient variability of the datasets included in this study, it was possible to identify an interesting relationship between their variability and the possible levels of accuracy to be obtained by the vegetation indices. When the biomass variability is only about twice the variability of the nutrient, the N_1645_1715 VI model was able to accurately predict the nutrient concentration. In comparison, when the biomass variability was 3 or more times higher, the accuracy decreased significantly, illustrating the high effect of biomass in the spectral response. This effect was confirmed when testing the VIs for monitoring the total content of both potassium and phosphorus, showing a significant improvement accuracy of both the VIs and the PLS models. These results show that in order to retrieve a better accuracy in the prediction of the nutrient concentration, it is needed to first retrieve the biomass from the spectral information so to then compute the nutrient concentration from the VI model. Our findings suggest the possibility of including the wavelengths of this proposed VI in the design of future multi or superspectral resolution satellites.

Acknowledgements

This research was supported by the Dead Sea Works Ltd. The authors thank the support given by Dr. Patricia Imas (DSW) and by Dr. Bansal's team from the Potash Research Institute of India, for their invaluable help in coordinating and performing the field Indian campaign. In addition, the authors want to specially thank all the farmers from Sohna (India) and Mishmar HaNegev (Israel) for their invaluable help during the field campaigns and for allowing the collection of samples from their lands without demanding any compensation.

References

Aparicio, N., Villegas, D., Araus, J., Casadesus, J., Royo, C., 2002. Relationship between growth traits and spectral vegetation indices in Durum wheat. Crop Sci. 42, 1547–1555.

Ayala-Silva, T., Beyl, C.A., 2005. Changes in spectral reflectance of wheat leaves in response to specific macronutrient deficiency. Adv. Space Res. 35 (2), 305–317.

Baret, F., Guyot, G., 1991. Potentials and limits of vegetation indices for LAI and APAR assessment. Remote Sens. Environ. 35 (2–3), 161–173.

Birth, G.S., McVey, G.R., 1968. Measuring the color of growing turf with a reflectance spectrophotometer. Agron. J. 60 (6), 640–643.

Bonfil, D., Mufradi, I., Klitman, S., Asido, S., 1999. Wheat grain yield and soil profile water distribution in a no-till arid environment. Agron. J. 91 (3), 368–373.

Bowker, D., Davis, R., Myrick, D., Stacy, K., Jones, W., 1985. Spectral Reflectances of Natural Targets for Use in Remote Sensing Studies. NASA, Washington, DC, Ref. Pub. 1139.

Buschmann, C., Nagel, E., 1993. In vivo spectroscopy and internal optics of leaves as basis for remote sensing of vegetation. Int. J. Remote Sens. 14 (4), 711–722.

Cohen, Y., Alchanatis, V., Zusman, Y., Dar, Z., Bonfil, D.J., Karnieli, A., Zilberman, A., Moulin, A., Ostrovsky, V., Levi, A., Brikman, R., Shenker, M., 2009. Leaf nitrogen estimation in potato based on spectral data and on simulated bands of the VENμS satellite. Precision Agric. 11 (5), 520–537.

Curran, P., 1989. Remote sensing of foliar chemistry. Remote Sens. Environ. 30, 271–289.

Filella, I., Serrano, L., Serra, J., Penuelas, J., 1995. Evaluating wheat nitrogen status with canopy reflectance indices and discriminant analysis. Crop Sci. 35, 1400–1405.

Fridgen, J.L., Varco, J.J., 2004. Dependency of cotton leaf nitrogen, chlorophyll, and reflectance on nitrogen and potassium availability. Agron. J. 96 (1), 63–69.

Gitelson, A., Kaufman, Y., Merzlyak, M., 1996. Use of a green channel in remote sensing of global vegetation from EOS-MODIS. Remote Sens. Environ. 58 (3), 289–298.

Gomez-Casero, M.T., Lopez-Granados, F., Pena-Barragan, J.M., Jurado-Exposito, M., Garcia-Torres, L., Fernandez-Escobar, R., 2007. Assessing nitrogen and potassium deficiencies in olive orchards through discriminant analysis of hyperspectral data. J. Am. Soc. Hort. Sci. 132 (5), 611–618.

Guyot, G., Baret, F., 1988. Utilisation de la haute resolution spectrale pour suivre l'etat des couvrets vegetaux. In: 4th International Colloquium on Spectral Signatures of Objects in Remote Sensing. ESA SP-287 , Aussois, France, pp. 279–286.

Haboudane, D., Miller, J., Tremblay, N., Zarco-Tejada, P., Dextraze, L., 2002. Integrated narrow-band vegetation indices for prediction of crop chlorophyll content for application to precision agriculture. Remote Sens. Environ. 81 (2–3), 416–426.

Hansen, P., Schjoerring, J., 2003. Reflectance measurement of canopy biomass and nitrogen status in wheat crops using normalized difference vegetation indices and Partial Least Squares regression. Remote Sens. Environ. 86 (4), 542–553.

Hatfield, J.L., Gitelson, A.A., Schepers, J.S., Walthall, C.L., 2008. Application of spectral remote sensing for agronomic decisions. Agron. J. 100, S-117-131.

Herrmann, I., Karnieli, A., Bonfil, D.J., Cohen, Y., Alchanatis, V., 2010. SWIR-based spectral indices for assessing nitrogen content in potato fields. Int. J. Remote Sens. 31 (19), 5127–5143.

Huete, A., 1988. A soil-adjusted vegetation index (SAVI). Remote Sens. Environ. 25 (3), 295–309.

Knipling, E., 1970. Physical and physiological basis for the reflectance of visible and near-infrared radiation from vegetation. Remote Sens. Environ. 1, 155–159.

Jones, J., Case, V., 1990. Sampling, handling, and analyzing plant tissue samples. In: Soil Testing and Plant Analysis. SSSA, Inc., Madison, WI, pp. 389–427.

Nguyen, H., Lee, B., 2006. Assessment of rice leaf growth and nitrogen status by hyperspectral canopy reflectance and Partial Least Square regression. Eur. J. Agron. 24 (4), 349–356.

Osborne, S., Schepers, J., Francis, D., Schlemmer, M., 2002. Detection of phosphorus and nitrogen deficiencies in corn using spectral radiance measurements. Agron. J. 94, 1215–1221.

Petersen, C.T., Jensen, C.R., Mogensen, V.O., 2002. Analysis of variation of spectral vegetation index measured in differently fertilized field barley. Commun. Soil Sci. Plant Anal. 33 (9/10), 1485–1506.

Pimstein, A., Eitel, J.U., Long, D.S., Mufradi, I., Karnieli, A., Bonfil, D.J., 2009. A spectral index to monitor the head-emergence of wheat in semi-arid conditions. Field Crops Res. 111 (3), 218–225, doi:10.1016/j.fcr.2008.12.009.

Pimstein, A., Karnieli, A., Bonfil, D.J., 2007. Wheat and maize monitoring based on ground spectral measurements and multivariate data analysis. J. Appl. Remote Sens. 1, 013530, doi:10.1117/1.2784799.

Ponzoni, F.J., Goncalves, J.L.D.M., 1999. Spectral features associated with nitrogen, phosphorus, and potassium deficiencies in *Eucalyptus saligna* seedling leaves. Int. J. Remote Sens. 20, 2249–2264.

Rouse, J., Haas, R.H., Schell, J.A., Deering, D.W., 1974. Monitoring vegetation systems in the Great Plains with ERTS. In: 3rd Earth Resources Technology Satellite-1 Symposium, NASA SP-351 , Greenbelt, MD, pp. 301–317.

Samborski, S.M., Tremblay, N., Fallon, E., 2009. Strategies to make use of plant sensors-based diagnostic information for nitrogen recommendations. Agron. J. 101, 800–816.

Seelan, S., Laguette, S., Casady, G.M., Seielstad, G.A., 2003. Remote sensing applications for precision agriculture: a learning community approach. Remote Sens. Environ. 88 (1–2), 157–169.

Stanhill, G., Kafkafi, U., Fuchs, M., Kagan, Y., 1972. The effect of fertilizer application on solar reflectance from wheat crop. Israel J. Agric. Res. 22 (2), 109–118.

Tisdale, S., Nelson, W., Beaton, J., 1985. Soil Fertility and Fertilizers. Macmillan Publishing Company, New York.

Wallace, T., 1943. The Diagnosis of Mineral Deficiencies in Plants by Visual Symptoms. His Majesty's Stationary Office, London, http://www.hbci.com/~wenonah/min-def/index.html. (Accessed 30 11 2010).